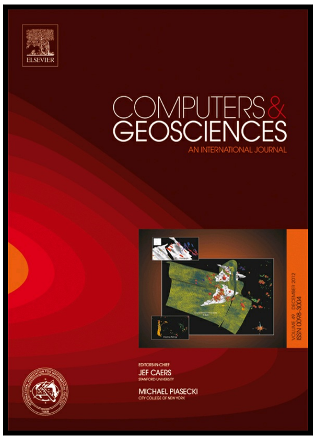

www.elsevier.com/locate/cageo

Vel-IO 3D: A tool for 3D velocity model construction, optimization and time-depth conversion in 3D geological modeling workflow

Francesco E. Maesano, Chiara D'Ambrogi

PII: S0098-3004(16)30729-4
DOI: http://dx.doi.org/10.1016/j.cageo.2016.11.013
Reference: CAGEO3873

To appear in: *Computers and Geosciences*

Received date: 7 April 2016
Revised date: 22 September 2016
Accepted date: 28 November 2016

Cite this article as: Francesco E. Maesano and Chiara D'Ambrogi, Vel-IO 3D: A tool for 3D velocity model construction, optimization and time-depth conversio in 3D geological modeling workflow, *Computers and Geoscience*, http://dx.doi.org/10.1016/j.cageo.2016.11.013

Vel-IO 3D: a tool for 3D velocity model construction, optimization and time-depth conversion in 3D geological modeling workflow.

Francesco E. Maesano[a*], Chiara D'Ambrogi[b]

[a]INGV – Istituto Nazionale di Geofisica e Vulcanologia, Via di Vigna Murata 605, 00143 Roma. Previously at ISPRA – Servizio Geologico d'Italia, Via Vitaliano Brancati 48, 00144, Roma

[b]ISPRA – Servizio Geologico d'Italia, Via Vitaliano Brancati 48, 00144, Roma

*Corresponding Author. Francesco E. Maesano. INGV, Istituto Nazionale di Geofisica e Vulcanologia, Via di Vigna Murata 605, 00143, Roma, Italy. Tel.: +393805164993. email: francesco.maesano@ingv.it

Abstract

We present Vel-IO 3D, a tool for 3D velocity model creation and time-depth conversion, as part of a workflow for 3D model building. The workflow addresses the management of large subsurface dataset, mainly seismic lines and well logs, and the construction of a 3D velocity model able to describe the variation of the velocity parameters related to strong facies and thickness variability and to high structural complexity. Although it is applicable in many geological contexts (e.g. foreland basins, large intermountain basins), it is particularly suitable in wide flat regions, where subsurface structures have no surface expression.

The Vel-IO 3D tool is composed by three scripts, written in Python 2.7.11, that automate i) the 3D instantaneous velocity model building, ii) the velocity model optimization, iii) the time-depth conversion. They determine a 3D geological model that is consistent with the primary geological constraints (e.g. depth of the markers on wells).

The proposed workflow and the Vel-IO 3D tool have been tested, during the EU funded Project GeoMol, by the construction of the 3D geological model of a flat region, 5 700 km^2 in area, located in the central part of the Po Plain. The final 3D model showed the efficiency of the workflow and Vel-IO 3D tool in the management of large amount of data both in time and depth domain. A 4 layer-cake velocity model has been applied to a several thousand (5 000 - 13 000 m) thick succession, with 15 horizons from Triassic up to Pleistocene, complicated by a Mesozoic extensional tectonics and by buried thrusts related to Southern Alps and Northern Apennines.

Keywords: 3D geological modeling; 3D velocity model; Po Plain; Time-depth conversion; Velocity analysis

1. Introduction

Despite their wide use, geological 3D modeling techniques in wide flat regions, where “the essential is invisible to the eye” (de Saint-Exupéry, 1943) have unresolved issues. These include the quality of subsurface data and the total lack of outcrops as constraints, to the management of great amounts of subsurface data, mainly seismic reflection profiles, and their time-depth conversion to be usefully integrated with well logs or other geological constraints in the depth domain, as well as the representation of the uncertainties.

Accordingly, in the past decades authors have chiefly investigated and refined techniques and workflows to build 3D models that rely mainly on surface data, require the projection at depth of the derived geometrical constraints and integrate the reconstruction with well logs or seismic lines, if available (Baumberger, 2015; Bistacchi et., 2008; Kaufmann and Martin, 2008; Svennevig et al., 2015; Zanchi et al., 2009). Almost only the oil and gas industry developed methods to manage and optimize subsurface geological and geophysical data to obtain consistent 3D geological models, without outcrop data.

However wide flat regions are often both strategic and critical areas due to the strong anthropogenic pressure and energy needs, connected with big cities, critical infrastructures and industrial facilities. The ability to consistently describe and model in three-dimensions the subsurface geological structures, that host natural resources (e.g. groundwater, oil and gas, geothermal energy, CCS and natural gas storage), and at the same time generate and control geohazards (e.g. earthquake, vertical ground movement), underpins any further analysis and application in these areas.

We have designed a workflow for 3D model production only from subsurface data, which core is Vel-IO 3D, a tool developed in ArcGIS; it allows the management of velocity data, the calculation of a 3D instantaneous velocity model, that are the most difficult steps for the 3D model building in wide flat regions with dense and consistent subsurface dataset in the time domain, and the time-depth conversion. The time-depth conversion techniques usually available in commercial software are largely based on average or interval velocity values; this approach returns results that can be adequate for small areas with quite constant unit thickness but it is not enough satisfactory to produce 3D model of wide areas characterized by strong lateral velocity variations controlled by lithological heterogeneities and variability of the unit thicknesses.

The workflow and the Vel-IO 3D tool have been tested in the central Po Plain, identified as an ideal case study for its geological characteristics and for the great availability of subsurface data there.

2. Material and methods

3D modeling of subsurface structures in wide flat regions can be realized only if underground data are available; well logs and seismic reflection profiles are needed to overcome the total absence of outcrops and surface data, generally used as input data and geometrical constraints in the most common 3D modeling workflows.

Although generally these data are scarcely available or accessible (for industrial or legal restrictions), in flat densely populated areas, with high geo-potentials and affected by natural hazards, the occurrence of large amount of data, such as seismic reflection profiles or well logs , gravity data, seismological data, GPS or SAR measurements, is facilitated.

2D seismic reflection profiles, well stratigraphies with associated petro-physical parameters (e.g. velocity, resistivity, SP and acoustic logging), and stacking velocities obtained from processing of seismic lines, are the basic input data of the proposed 3D modeling workflow. The integration of these data, characterized by a different domain of the Z axis (time and depth), passes through the analysis of velocity data and the construction of a 3D velocity model for the time-depth conversion. To properly manage this critical phase of the 3D model construction we developed the Vel-IO 3D tool as core part of our 3D modeling workflow.

The designed workflow (Fig. 1), implemented after Maesano et al. (2014), is articulated in two different domains of the Z axis: time and depth; each one characterized by separate steps, sometimes connected to check the validity and consistency of the analysis and elaboration. After the time-depth conversion of the 3D model the steps are completely developed in the depth domain. Whereas the general workflow proposed here can be used in any geological context where the same type of data are available, the Vel-IO 3D tool has been designed specifically to be applied in wide flat regions or in offshore areas. As a matter of fact, in its present form, it does not account for the topography reference in the velocity model building and time-depth conversion.

2.1 Workflow

The main phases of the workflow can be summarized as follow:

1. Data: harmonization and interpretation;

2. Elaboration of the 3D model in time domain;
3. Calculation of the 3D velocity model;
4. 3D model time-depth conversion;
5. Consistency check and refinement of the 3D model in depth domain;
6. Construction of the final 3D model and parameterization.

2.1.1 Data: harmonization and interpretation

The input data used in the 3D modeling workflow are mainly constituted by: time migrated 2D seismic lines, well stratigraphies and associated petro-physical parameters (especially sonic log), stacking velocities obtained from processing of seismic lines.

The harmonization process, as a key to transform the different data sets in such a way they fit together both with respect to geometry and semantics, is guided by an unified stratigraphic scheme. The scheme defines lithostratigraphic units and their regional boundaries (e.g. unit top or unconformity/relative conformity surfaces) (Fig. 2A) taking into account the detail needed for the further applications of the 3D model, and is the base reference for seismic and well data interpretation.

The well data are digitized and stored in a database; they are marked by some primary keys (e.g. seismic unit, formation, age), that enable the correlation between well logs and data deriving from the seismic picking. This integrated approach supports the check of the line drawing during seismic interpretation, using a swift depth-time conversion of the well markers.

Moreover the velocity data from well logs are stored to be further analyzed and support the 3D velocity model construction (Fig. 2B).

2.1.2 Elaboration of the 3D model in time domain

The first step of the modeling is the construction of the 3D model in time based on the picked points, from seismic reflection lines interpretation (Fig. 3), referred to each horizons (unit top or unconformity surface). The Delaunay triangulation is the method chosen to obtain a raw preliminary 3D model because the triangulation i) honors all the input points, ii) optimizes the geometry of the triangles and iii) fulfils the nearest neighbor relation. The raw 3D model in time includes also the fault surfaces interpolated, with the same method, from the fault segments assigned to a specific fault system during the seismic interpretation.

The surfaces of the preliminary 3D model in time are resampled, to obtain a regular distribution of points, using a gridding procedure that allows to control the orientation and size of the grid, and to manage the resampling of high-inclined surfaces (e.g. reverse faults, sub-vertical surfaces). The procedure uses inclined grids, one for each surface in the preliminary model, with dip and azimuth defined to obtain the best fit on azimuth and dip of the surface to be resampled. The size of the grid cells is defined by the user according to the distribution of the input data and to the applications expected for the final 3D model.

The points of gridded surfaces are the input data for the time-depth conversion.

2.1.3 Calculation of the 3D velocity model and 3D model time-depth conversion

The procedure for this crucial step originated from the time-depth conversion tool of MOVE^{tm} (Midland Valley Ltd.) and its background theory (Etris et al., 2001); however we modified it to overcome the limitation of a time-depth conversion based on unique set of velocity parameters for each key horizon, which can be a major problem in areas with significant facies and thickness variations.

Starting points of our procedure are: i) the choice of the key horizons for the velocity model (Fig. 2A), and ii) the velocity parameters and their spatial variation, for each of the key horizons.

The velocity data are provided by well sonic logs, converted in interval velocities (Fig. 2B) measured each 100 m (in average), as well as pseudo-wells used to densify, if needed, the inhomogeneous distribution of interval velocities data. The pseudo-wells are derived from the analysis of stacking velocities obtained from processing of seismic lines. The reliability of pseudo-wells was tested by comparing their velocity profiles with adjacent well logs provided with velocity data.

A detailed description of this step, including the Vel-IO 3D tool, is in the paragraph **2.2 3D velocity model and time-depth converter: theory and calculation,** and in the Supplementary materials 1.

Whenever the points in the time domain represent the nodes of the surfaces built in the 3D environment (e.g. Move software), after the time-depth conversion procedure they can be re-imported into the 3D environment as meshes with preserved boundaries (Fig. 4); no further basic editing is needed except those connected with the model consistency check and refinement (see paragraph 2.1.4).

2.1.4 Consistency check, refinement and integration of the 3D model in depth domain

The points obtained after the time-depth conversion represent the input data to build the 3D model in depth.

This phase of the workflow is devoted to:

1) checking the consistency of surfaces;

2) the refinement and integration of the model with new inferred elements, mainly faults.

The first phase is the general overview of the model consistency to verify, and eventually correct, the depth of the horizons and their stratigraphic relationship (e.g. inconsistent position of older vs younger horizons, anomalous topography intersection, unconformities cut by eroded horizons).

To adjust the major differences or errors the following actions are possible: i) a further run of seismic interpretation; ii) a reshape of the areas with the residual misfits.

After this phase the model is refined checking the following aspects:

1) depth comparison of the surfaces not used as key horizons in the velocity model and time-depth conversion: the well log markers define depth constraints that are used to reshape the relevant surfaces in the 3D model;

2) addition of horizons, not picked during seismic interpretation, using thickness values from the well log stratigraphies;

3) critical revision of the displacement of each horizon through faults, in accordance with their kinematics;

4) correct hierarchical relationship between faults and validate the interpretation of poor data-constrained areas, also comparing them with independent data (e.g. gravity anomalies, HVSR measurements) (ISPRA, 2015; Tarabusi and Caputo, 2016);

5) comparison of the surface trends and morphological discontinuities with the position of fault surfaces;

6) addition of inferred faults on the base of a spatial analysis of horizon surfaces and/or abrupt changes in the direction of modeled faults.

The inferred faults are generally high angle faults, oriented parallel to the trend of the seismic lines, not easily detectable during seismic interpretation, but essential for the description and characterization of structural systems (e.g. segmentation of the thrusts, wrong correlation of fault segments).

2.1.5 Construction of the final 3D model and parameterization

In the end, the 3D model is refined and the surfaces are resampled , with the same gridding procedure described in paragraph 2.1.2, using grids with the best fit on the azimuth and dip of each surfaces, and a spacing adequate to the final use of the model. At this step final surfaces in the model (unit tops, unconformities and faults) can be used to build volumes of the most relevant units (e.g. aquifers, reservoirs). Both surfaces and volumes can be populated with petro-physical parameters derived from the well log database (e.g. temperature, porosity, permeability, mineralization) or other data sources, to be further used for other applications.

2.2 Vel-IO 3D tool: theory and calculation

The 3D velocity model and time-depth conversion of the 3D model in time domain are the key steps for the production of the final three-dimensional model.

The necessary requisite for the time-depth conversion is the construction of a model of the velocities at which the seismic waves propagate in the subsurface to be applied to all the objects included in the time-domain model.

To build the velocity model, various methodological approaches and strategies can be adopted, based on different type of velocities (i.e. stacking, normal-moveout (NMO), root-mean-square (rms), average, interval, and instantaneous) (Yilmaz, 2001):

- Average interval velocities from well logs;
- Grid of interval and stacking velocities;
- 3D grid with double velocity model;
- 3D grid with average velocities;
- 3D grid with interval velocities;
- 3D instantaneous velocity model.

The choice of the best strategy depends on the objective of the study and on the use of the final depth converted objects. For these reasons the velocity model building must take into account that:

1) the final depth-converted model must be geologically consistent;

2) it must be optimized for the resolution needed to resolve the geological complexity of the study area and for the subsequent applications;

3) it must include all the available velocity data, harmonized to be comparable, and properly weighted.

In this paper we present the construction of a 3D instantaneous velocity model to be applied in wide areas characterized by great level of geological complexity (i.e. presence of inherited faults, multiphase deformations, syntectonic deposition, important lateral thickness variations).

The main characteristic of an instantaneous velocity model is that it takes into account the variability of velocity with depth. In general, the average velocity tends to increase with increasing depth due to the compaction related to lithostatic load. Nevertheless, within individual geological units, the velocity variation can behave in different ways and sometimes velocity inversion (sudden back step of the velocity trend from one body to another or decrease of velocity with depth) can occur. These latter cases can be managed better with an instantaneous velocity model, instead of an interval or average velocity model, because it better describes the behavior of the velocity inside a geological body (Etris et al, 2001).

A preliminary step for the construction of the velocity model is the analysis of the velocity data within the area; these data are provided by sonic logs and from stacking velocities obtained from seismic processing.

Pseudo-wells could be built, if needed, aggregating the interval stacking velocities, of adjacent traces (on one or more intersecting seismic lines) in order to perform a more consistent statistical analysis of velocity (Etris et al., 2001). Since the stacking velocities are provided in time domain (Time - Velocity curve), they need to be converted in depth domain along the pseudo-well in order to make them comparable with the well logs velocity data (Depth – Velocity curve).

The well log analysis leads to the choice of the main geological layers, and related key horizon boundaries, within which the velocity behavior can be considered homogeneous. The depth variations of all the velocity values (e.g. interval velocities) within a defined layer are plotted in a graph to search a single f(Z) function that can describe the velocity variation within a confidence interval of linear regression, following a methodological approach similar to that proposed by van Dalfsen et al. (2006).

Numerous velocity functions have been proposed in literature (Alaminiokuma and Ugbor, 2010; Al-Chalabi, 1997) to describe the velocity variation with depth; in this study, we used the linear function (Eq. 1).

$$v(Z) = v_0 + kZ \quad (1)$$

Where v(Z) is the velocity (m/sec) at Z depth (m) and v_0 and k (1/sec) are respectively the initial velocity at the top of the considered layer (i.e. at the key horizon) and the gradient describing the velocity variations with depth (Ravve and Koren, 2006) (Fig. 5A).

The depth of each point within a key horizon is described by the following equation proposed by Marsden (1992):

$$Z_n = Z_{n-1} + v_{0n} (e^{k_n t_n} - 1)/k_n \quad (2)$$

Where Z_{n-1} is the depth (m) of the key horizon directly above the analyzed point, v_{0n} is the initial velocity (m/sec) of the layer in which the point is located, k_n is the gradient of the layer in which the point is located and t_n is defined as:

$t_n = (twt_n – twt_{n-1})/2\ 000$

Where twt_n is the two-way traveltime (in msec) of the point to convert, and twt_{n-1} the two-way traveltime of the corresponding point on the key horizon directly above; the division for 2 000 convert the two-way traveltime to one-way traveltime and from msec to seconds. Following the example in Fig. 5B, the depth of the point "a", located in an intermediate position between two key horizons, will be:

$Z_a = Z_1 + v_{02}\ (e^{k2ta} – 1)/k_2$

With $t_a = (twt_a – twt_1)/2\ 000$

This methodology for depth conversion is already used by default in the 3D kinematic modeling module of Move^{tm} with two major limitations: i) to consider a single value of velocity and gradient for each horizon in the model, ii) do not consider the presence of physical boundaries (e.g. major faults) separating domains with different velocity properties. These restrictions imposed by Move leads to an oversimplification of the velocity model not accounting for lateral variabilities.

To overcome this problem, especially when the 3D models are related to wide and complex areas, we implemented a tool, mainly based on ESRI ArcGIS tools for Spatial Analysis and interpolation, as core of the modeling workflow.

This procedure for the velocity model building and the time-depth conversion has been synthesized in three Python scripts, the Vel-IO 3D (Fig. 6), that can be used independently (see Supplementary materials 1 for a detailed description and Supplementary materials 2 for the code).

The scripts were written in Python 2.7.11, using arcpy and itertools modules and need ArcMap 10.3 or above with Spatial Analyst extension license. The three scripts perform different tasks:

1) 3D instantaneous velocity model building;
2) Velocity model optimization;
3) Depth conversion.

The idea behind the three scripts is to assign the velocity model parameters to each point of X and Y coordinates within the 3D model in time domain and then perform the calculation of the depth value.

2.2.1 Script 1 - 3D instantaneous velocity model builder

The Vel-IO 3D Script 1 (Supplementary materials 1, Fig. S1) creates a preliminary 3D instantaneous velocity model using the information on the shape of the key horizons in time domain and the velocity data (v_0 and k) obtained from the analysis of well and pseudo-well logs. The script applies spatial interpolation (Inverse Distance Weighted as default method, refers to Supplementary materials 1 for details) to the velocity parameters, and extraction algorithms to calculate, step by step, the value of depth of each point on key horizons using the Marsden equation.

The outputs of this script, for each key horizon, are raster grids with the interpolated values of v_0 and k across the study area, and the shape of the horizon in time and depth domain.

2.2.2 Script 2 - Velocity model optimizer

The Vel-IO 3D Script 2 (Supplementary materials 1, Fig. S2) is designed to improve the consistency of the velocity model obtained after the Script 1, adding new v_0 and k values derived from measured depths, thus reducing the geometrical uncertainties in the areas located far from the original velocity data (optimization). The main goals of this script are: i) to perform a sanity check of the results of Script 1 using independent data and ii) to infer velocity and gradient information for additional points (control points) represented by wells stored within the database, but not provided with velocity data.

The velocity analysis and interpolations performed in the Script 1 are used to calculate the standard deviation of v_0 and k within each key horizon inside the study area. Using this range of variability as the upper and lower boundaries of search, the Script 2 finds the best values of v_0 and k that are needed to obtain a calculated depth (Z) with the minimum difference from the measured depth (Z_{cp}) in the control points for each horizons (Fig. 7).

If the residual difference is higher than a given tolerance threshold (e.g. the vertical resolution of the seismic profiles used during the interpretation), the script returns a warning. The warnings can be used to check if in correspondence of the control points there is a mismatch with the original interpretation.

The best v_0 and k values found for each horizon during the optimization are then associated to the control points coordinates and are used, together with the existing velocity data, to calculate optimized grids of the velocity model.

2.2.3 Script 3 - Time-Depth converter

The Vel-IO 3D Script 3 (Supplementary materials 1, Fig. S3) runs the time-depth conversion of any object located inside the 3D velocity model and can run independently from the other two scripts (e.g. a velocity model obtained with other methods can be used to perform the time-depth conversion with Script 3).

The input data are the velocity model and the points in time domain describing the shape of the objects to be depth converted. The points can represent any horizon within, or transverse, to the key horizons (e.g. faults and lithofacies transitions) in the 3D velocity model. Multiple objects can be depth converted at the same time if they are stored with an attribute referring to the object name. The Script 3 calculates the position of each point with respect to the key horizons of the velocity model and then it performs the time-depth conversion using the Marsden equation.

3. Test area

The proposed workflow and Vel-IO 3D tool have been tested for the construction of the 3D geological model of a flat region, 5 700 km^2 in area, located in the central part of the Po Plain (Fig. 8A) (ISPRA, 2015). The 3D model was built in the framework of the European funded Project GeoMol.

3.1 Geological setting

The Po Plain is the common foreland of two facing mountain chains: the Southern Alps, to the north, and the Northern Apennines, to the south. A compressional tectonic, N-S oriented, superimposed to the previous Mesozoic extensional tectonics-related framework, involved first (Middle Eocene-Miocene) the Southern Alps, and then, with an NNE-SSW orientation, also the Northern Apennines (from the Oligocene). The resulting contractional structures are the Southern Alps Thrust Front and three arcs, along the external margin of the Northern Apennines, from west to east: i) Monferrato Arc, ii) Emilia Arc; iii) Ferrara-Romagna Arc (Fig. 8A).

The Apennines-related flexural subsidence (Scrocca et al., 2007) and fast sedimentation rate (Bartolini et al., 1996; Maesano and D'Ambrogi, 2016; Mancin et al., 2009) produced the burial, with few exceptions, of the growing structures of both Southern Alps and Northern Apennines and the filling of the basin with an up to 8 000 meters thick Plio-Pleistocene succession (Ghielmi et al., 2013; Pieri and Groppi, 1981).

The oldest part of the stratigraphic succession consists of continental clastic deposits of Middle Permian age, passing to Lower Triassic carbonate platform units (Fig. 2A). An intense synsedimentary extensional tectonics controlled the complex paleogeographic setting defining intra-platform through, and from Late Triassic deeper basins between shallow marine carbonate platform areas (Bertotti et al., 1993; Fantoni and Franciosi, 2010). During Cenozoic, units of the Southern Alps and Northern Apennines foredeeps were deposited, followed by a regressive sequence of Quaternary shallow marine and continental sediments (Argnani and Ricci Lucchi, 2001; Dondi and D'Andrea, 1986; Ghielmi et al., 2010).

The structural style of the fold-and-thrust belts was controlled by two major detachment levels (Fig. 2A), one located at the base of the Mesozoic carbonate units, within the Triassic evaporites, and a shallower one in the upper Oligocene to lower–middle Miocene deposits.

This complex structural and sedimentary history produced strong lateral and vertical facies and thickness variations, and sharp contacts across faults and repetitions.

3.2 3D model

A dense dataset of seismic lines (12 000 km) and exploration wells (130 drilling), mainly deriving from the oil and gas exploration activity carried out over the past 60 years across the entire Po Plain, (Fig. 8B) (ISPRA, 2015), forms the foundation for the 3D model.

The main objectives of the 3D model were to support the geo-resources assessment (GeoMol Team, 2015), in particular the geothermal potential, and the better definition of the seismotectonics of the area with refinement of the previously known seismogenic sources (DISS Working Group, 2015).

The seismic lines were acquired from the 1952 to 1991 and were reprocessed by ENI S.p.A. within the scope of its exploration and production projects; the maximum two-way traveltime recorded is 8 000 msec.

The wells, drilled from the 1930 to 2004, range from 700 to 7 100 meters of maximum depth, with a mean value of 2 300 meters. The logs contain petro-physical parameters, at least lithology and age, but not always porosity, permeability, velocity.

The seismic interpretation and the harmonization of well log stratigraphies followed a regional stratigraphic scheme consisting of 15 horizons from Triassic up to Pleistocene and of two main decollement levels (L1 and L2) (Fig. 2A). During the seismic interpretation and line drawing (Fig. 3), particular attention has been addressed to the precise, as much as possible, definition of the fault upper tip position (intended as: i) depth of the tip and ii) identification of the younger faulted horizon); this information is a pivotal for the age of inception of the fault activity.

The 3D model in the time domain originated from more than 2 500 000 picked points and consisted of 76 surfaces related to 13 horizons and more than 150 faults. Maps showing the density of points picked during seismic interpretation and including well markers have been published, for each of the modeled horizon, in ISPRA (2015).

This model has been depth converted using the previously described procedure, with a 4 layer-cake 3D velocity model (Fig. 2A and Fig. 9).

The 4 layers were chosen on the basis of the rock type and of their average thickness, in order to have enough interval velocity counts to perform a statistical analysis in each well. The two uppermost layers (Layer 1 and Layer 2) represent the Plio-Pleistocene siliciclastic infilling of the Northern Apennines foredeep. Layer 3 includes the Southern Alps coarse foredeep deposits and their heteropic distal units. The deeper layer (Layer 4) represents the Meso-Cenozoic carbonate units.

The structural complexity of the area has been taken into account, during the interpolation, using the major faults as barriers (Fig. 9) delimiting sub-areas of statistical consistency of velocity parameters.

The final 3D velocity model is summarized in the 4 maps of Fig. 9 showing the distribution of the velocity data, the spatial variability of the initial velocity (v_0) and the contouring of the velocity gradient (k) for each key horizon inside the area.

The distribution of the input velocity data, from well logs and pseudo-wells, helps assess the inherent uncertainty of the velocity model. As a general rule, one might assume that the uncertainty increases as depth of the key horizon increases and as the number of wells and pseudo-wells decreases.

The central part of the area is a good example of the trade-off between structural complexity and input data in addressing the uncertainty of the resulting 3D model; this area has a fewer number of input data but a much simpler geological structure (the so-called Mantova Monocline, Ghielmi et al., 2013), therefore one may deduce that its overall uncertainty is not necessarily higher than the uncertainty of the rest of the model.

All the initial velocity maps show a central portion with an homogeneous increase of the velocity from NE to SW following the Mantova Monocline. The areas at the hangingwall of the main thrusts show more complex velocity trends with local minima generally located in the more prominent structural highs.

The gradient values are generally higher in the correspondence of the initial velocity minima (i.e. in the structural highs and in the NE part of the Mantova Monocline) indicating a higher velocity increase with depth where the initial velocities are lower.

This trend is particularly evident in the Ferrara Arc, delimited, during the velocity interpolation, by two barriers: one in the frontal part (representing the envelop of the major frontal thrusts) and one in the rear, where back-thrusts are well developed. The area beside the Ferrara Arc shows less variability both in the initial velocity values and in the gradient, especially for Layer 1 and Layer 2.

After the time-depth conversion the model has been completed by two horizons in layer 4 (MAI and NOR, in Fig. 2A) derived from a thickness analysis of the units K-PAL and J-K (Fig. 2A) on well logs and built on the basis of the SCA reference key horizon.

The final model contains 128 surfaces related to the 15 horizons (Fig. 2A), covering the entire study area (except for the erosional or non depositional areas), and 178 faults with length up to 1 000 m. The vertical extent of the model ranges from 5 000 m to 13 000 m (Fig. 10).

The great amount of available input data and the workflow adopted for the 3D model construction, with optimization of the velocity data used for the 3D velocity model and time-depth conversion (Vel-IO 3D), allow us to obtain an highly detailed 3D geological model at a regional scale. As a matter of fact the 3D model is consistent to describe a large number of stratigraphic and structural features, previously only partially or locally modeled (see Scardia et al., 2015; Livio et al., 2009; Bresciani and Perotti, 2015) or not modeled at all, such as (Fig. 10): i) extensional faults on the Mesozoic succession; ii) relations between thrusts with different detachment levels (L1 and L2), especially in the Southern Alps; iii) buried fault-related anticlines and their evolution through time; iv) 3D fault cut-offs and their upper tips. These elements can support many different applications such as the identification of buried active faults, and the calculation of sedimentation, uplift and slip rates (Maesano and D'Ambrogi, 2016).

4. Discussion and conclusions

The 3D modeling workflow with Vel-IO 3D tool proposed in this study for the time-depth conversion and the construction of the final 3D model has major impact on the shape of the horizons especially in the sectors where no velocity data or well markers are available. This implies that any further application performed using the 3D model as input data is directly affected from the initial assumption on the velocity model.

We perform two different analysis to validate our Vel-IO 3D tool.

A first analysis is based on Script 2, where the optimization is used not only to increase the number of values of v_0 and k in the velocity model, but also gives a quantitative evaluation of the difference between the predicted depth values (Z_c) and the measured depth in wells (Z_m) not used in the velocity model built by Script 1.

The second analysis was performed comparing the depth-converted surfaces with equivalent horizons mapped and published in literature.

Since there are no other publicly available 3D models in the Po Plain comparable for number of horizons and spatial extent with the model here presented, we could compare only the horizon Base PL of the GeoMol model with the equivalent surface of the base of Pliocene deposits available in literature from Structural Model of Italy (Bigi et al., 1992) (Fig. 11 A), that covers the entire Italian peninsula at 1:500 000 scale.

The horizon Base PL in our model (GeoMol model) is a regional unconformity easily recognizable along the basin margins, where it is also sampled by well logs, whereas it is more difficult to distinguish in the distal part of the basin.

In the commentary to the Structural Model of Italy (Bigi et al., 1992) there is no reference to the velocity model used, however considering the national extent of the mapped surface we may assume that an average velocity value was used.

To verify this hypothesis we: i) iterated the time-depth conversion of Base PL from the GeoMol Project using average velocities from 1 800 m/sec to 4 000 m/sec, with increasing steps of 200 m/sec; ii) calculated the difference in depth with the base of Pliocene from Bigi et al. (1992); iii) calculated the root mean square (RMS) residual at each step over the entire surface. We found that a velocity value of 3 000 m/sec allows to obtain the best fit with the surface of base of Pliocene from Bigi et al. (1992), with a residual RMS of 570 m. Then we compared the base of Pliocene of Bigi et al. (1992) with the Base PL of the GeoMol model time-depth converted with Vel-IO 3D. This comparison (Fig. 11 B) highlights a very close fit in the northern part of the study area (Southern Alps) and at the top of the Ferrara-Romagna Arc. Some differences, in the order of some hundreds meters, are located in the central part of the study area, at the footwall of the Ferrara-Romagna Arc, where they can be related both to the difficulties in the correlation of the unconformity and with the use of a different strategy for the time-depth conversion.

However moving to the south of the Ferrara-Romagna Arc, in the depocenter between Ferrara and Bologna, the discrepancies increase up to 2 000 meters (Fig. 11 C). We interpret these differences to be related to the different velocity model adopted for the time-depth conversion.

Since there is a significant variability of velocity between the top of anticlines of the Ferrara-Romagna Arc and other sectors (Fig. 9) (e.g. the foreland and the thrust-top basin depocenters) the use of a single velocity value can produce inconsistent geometries on the surface of base of Pliocene and also affects the geometry of the thrust-related anticline.

Considering the previous results on the comparison of the base of Pliocene surfaces it is possible to foresee the same influence of the velocity model on the other surfaces and to consider the subsequent effects on the further analyses based on the 3D model. This consideration points out the importance of the use of a 3D optimized instantaneous velocity model to obtain a 3D geological model consistent for applications that are deeply influenced by the accurate relative position and depth of the horizons and faults, such as:

- basin analysis based on sequential 3D restoration-and-decompaction workflow, that enables the calculation of sedimentation and uplift rates, and highlights the interaction of active tectonics and sedimentation (Maesano and D'Ambrogi, 2016);
- identification of active faults, also characterized by very elusive evidences of deformation of the syntectonic deposits, and slip rate calculation (Maesano et al., 2015);
- seismotectonic analysis with identification of new seismogenic sources, and better definition or modification of the existing ones (DISS working Group, 2015), characterized with 3D geometrical parameters.

Moreover a 3D velocity model strictly connected with the geological constraints is a fundamental input for any seismological studies such as relocating seismic events and simulation of ground motion shaking.

We present a comprehensive workflow for 3D model building in wide flat regions and offshore basins where raw data are stored in time and depth domain. The core of this workflow is the new Vel-IO 3D tool for 3D instantaneous velocity model construction and time-depth conversion that automatically optimize the available velocity data and the well log constraints.

The application of the whole workflow to a test area located in the Central Po Plain allowed the construction of a 3D geological model further used to support applications such as basin analysis, geopotential assessment, and seismotectonic studies.

WEB RESOURCES

http://www.geomol.eu - Homepage GeoMol Project “Assessing subsurface potential of the Alpine Foreland Basins for sustainable planning and use of natural resources

http://www.geomol.eu/mapviewer - GeoMol Mapviewer and WMS catalogue

http://www.geomol.eu/3dexplorer - GeoMol 3D interactive viewer and explorer

Acknowledgements

The seismic interpretation of the seismic dataset, kindly provided by ENI S.p.A., has been made by the authors and by the Italian GeoMol Team (A. Cagnoni, F.C. Molinari, E. Monesi, A. Piccin & G. Scardia).

Midland Valley Ltd is acknowledged for making available the Move software to ISPRA (2014-2015 ASI-Academic Software Initiative).

The Authors wish to thank R. Basili for the constructive discussions. The final version of the manuscript benefits from the suggestions and observations of two anonymous reviewers.

This research has been supported by the GeoMol Project "Assessing subsurface potential of the Alpine Foreland Basins for sustainable planning and use of natural resources" (project code 10-4-3-DE), co-funded by the Alpine Space Programme-European territorial Cooperation 2007-2013 (http://geomol.eu).

REFERENCES

Alaminiokuma, G.I., Ugbor, C.C., 2010. Analytical velocity model for depth conversion in the subsurface facies of Agbada Formation in the Niger Delta, Nigeria. The Pacific Journal of Science and Technology 11(1), 563-575.

Al-Chalabi, M., 1997. Time-Depth relationships for multiplayer depth conversion. Geophysical Prospecting 45, 715-720. DOI:10.1046/j.1365-2478.1997.520293.x

Argnani, A., Ricci Lucchi, F., 2001. Tertiary siliciclastic turbidite systems of the Northern Apennines. In: Vai, G.B., Martini, I.P. (Eds.), Anatomy Of An Orogen: The Apennines And Adjacent Mediterranean Basins. Springer, pp. 327-350.

Bartolini, C., Caputo, R., Pieri, M., 1996. Pliocene-Quaternary sedimentation in the northern Apennine foredeep and related denudation. Geological Magazine 133, 255-273.

Baumberger, R., 2015. Quantification of lineaments: Link between internal 3D structure and surface evolution of the Hasli valley (Aar massif, Central alps, Switzerland). Ph.D. Dissertation, Universität Bern, Switzerland, 132 pp.

Bertotti, G., Picotti, V., Bernoulli, D., Castellarin, A., 1993. From rifting to drifting: tectonic evolution of the South-Alpine upper crust from the Triassic to the Early Cretaceous. Sedimentary Geology 86, 53-76. doi: 10.1016/0037-0738(93)90133-P.

Bigi, G., Cosentino, D., Parotto, M., Sartori, R., Scandone, P., 1992. Structural model of Italy and gravity map, 1:500,000. Quad. Ric. Sci., 114, 3, S.EL.CA Florence.

Bistacchi, A., Massironi, M., Dal Piaz, G.V., Dal Piaz, G., Monopoli, B., Schiavo, A., Toffolon, G., 2008. 3D fold and fault reconstruction with an uncertainty model: An example from an Alpine tunnel case study. Computers & Geosciences 34(4), 351-372. doi:10.1016/j.cageo.2007.04.002

Bresciani, I., Perotti, C.R., 2014. An active deformation structure in the Po Plain (N Italy): the Romanengo anticline. Tectonics, 33(10), 2059–2076. doi:10.1002/2013TC003422 de Saint-Exupéry, A., 1943. Le Petit Prince. Reynal and Hitchcock, 93 pp.

DISS Working Group, 2015. Database of Individual Seismogenic Sources (DISS), Version 3.2.0: A compilation of potential sources for earthquakes larger than M 5.5 in Italy and surrounding areas. http://diss.rm.ingv.it/diss/, © INGV 2015 - Istituto Nazionale di Geofisica e Vulcanologia - All rights reserved; doi:10.6092/INGV.IT-DISS3.2.0

Dondi, L., D'Andrea, G., 1986. La Pianura Padana e Veneta dall'Oligocene superiore al Pleistocene. Giornale di Geologia Ser. 3 48(1-2), 197-225.

Etris, E.L., Crabtree, N.J., Dewar, J., 2001. True depth conversion: more than a pretty picture. Recorder 26(11), 11-22.

Fantoni, R., Franciosi, R., 2010. Tectono-sedimentary setting of the Po Plain and Adriatic foreland. Rendiconti Lincei 21(1), S197-S209. doi: 10.1007/s12210-010-0102-4.

GeoMol Team, 2015. GeoMol – Assessing subsurface potentials of the Alpine Foreland Basins for sustainable planning and use of natural resources. Project Report, 188 pp. (Augsburg, LfU), www.geomol.eu

Ghielmi, M., Minervini, M., Nini, C., Rogledi, S., Rossi, M., Vignolo, A., 2010. Sedimentary and tectonic evolution in the eastern Po-Plain and northern Adriatic Sea area from Messinian to Middle Pleistocene (Italy). Rendiconti Lincei 21(1), S131-S166. doi: 10.1007/s12210-010-0101-5.

Ghielmi, M., Minervini, M., Nini, C., Rogledi, S., Rossi, M., 2013. Late Miocene-Middle Pleistocene sequences in the Po Plain - Northern Adriatic Sea (Italy): The stratigraphic record of modification phases affecting a complex foreland basin. Marine and Petroleum Geology 42, 50-81. doi: 10.1016/j.marpetgeo.2012.11.007.

ISPRA, 2015. Modello geologico 3D e geopotenziali della Pianura Padana centrale (Progetto GeoMol). Rapporti ISPRA 234/2015, 104 pp. e Appendice [in Italian].

Kaufmann, O., Martin, T., 2008. 3D geological modelling from boreholes, cross-sections and geological maps, application over former natural gas storages in coal mines. Computers & Geosciences 34, 278–290. doi:10.1016/j.cageo.2007.09.005

Livio, F.A., Berlusconi, A., Michetti, A.M., Sileo, G., Zerboni, A., Trombino, L., Cremaschi, M., Mueller, K., Vittori, E., Carcano, C., Rogledi, S., 2009. Active fault-related folding in the epicentral area of the December 25, 1222 (Io=IX MCS) Brescia earthquake (Northern Italy): Seismotectonic implications. Tectonophysics, 476(1–2), 320–335. doi:10.1016/j.tecto.2009.03.019.

Maesano, F.E., and the Italian GeoMol Team, 2014. Integrating data sources for 3D modeling: the Italian activity in the GeoMol Project. Rend. Online Soc. Geol. It., 30, 28-32. doi: 10.3301/ROL.2014.07.

Maesano, F.E., D'Ambrogi C., Burrato P., Toscani G., 2015. Slip-rates of blind thrust in slow deforming area: Examples from the Po Plain (Italy). Tectonophysics 643, 8-25. doi: 10.1016/j.tecto.2014.12.007

Maesano, F.E., D'Ambrogi, C., 2016. Coupling sedimentation and tectonic control: Pleistocene evolution of the central Po Basin. Italian Journal of Geosciences 135(3). doi: 10.3301/IJG.2015.17

Mancin, N., Di Giulio, A., Cobianchi, M., 2009. Tectonic vs. climate forcing in the Cenozoic sedimentary evolution of a foreland basin (Eastern Southalpine system, Italy). Basin Research 21(6), 799-823. doi: 10.1111/j.1365-2117.2009.00402.x.

Marsden, D., 1992. V0-K Method for depth conversion. Leading Edge 11(8), 53-54.

Pieri, M., Groppi, G., 1981. Subsurface geological structure of the Po Plain, Italy. Progetto Finalizzato Geodinamica, Agip, (414), 1-13.

Ravve, I., Koren, Z., 2006. Exponential asymptotically bounded velocity model: Part I – Effective models and velocity transformations. Geophysics 71(3), 53-65. DOI:10.1190/1.2196033

Rossi, M., Minervini, M., Ghielmi, M., Rogledi, S., 2015. Messinian and Pliocene erosional surfaces in the Po Plain-Adriatic Basin: Insights from allostratigraphy and sequence stratigraphy in assessing play concepts related to accommodation and gateway turnarounds in tectonically active margins. Marine and Petroleum Geology 66(1), 192-216. doi: 10.1016/j.marpetgeo.2014.12.012.

Scrocca, D., Carminati, E., Doglioni, C., Marcantoni, D., 2007. Slab Retreat and Active Shortening along the Central-Northern Apennines. In: Lacombe, O., Roure, F., Lavé, J., Vergés, J. (Eds.), Thrust Belts and Foreland Basins. SE-25, Frontiers in Earth Sciences. Springer Berlin Heidelberg, pp. 471-487. doi: 10.1007/978- 3-540-69426-7_25.

Svennevig, K., Guarnieri, P., Stemmerik, L., 2015. From oblique photogrammetry to a 3D model - Structural modeling of Kilen, eastern North Greenland. Computers & Geosciences 83, 120-126. doi:10.1016/j.cageo.2015.07.008

Tarabusi, G., Caputo, R., 2016. The use of HVSR measurements for investigating buried tectonic structures: the Mirandola anticline, Northern Italy, as a case study. Int. J. Earth Sci. (Geol. Rundsch.). DOI 10.1007/s00531-016-1322-3 van Dalfsen, W., Doornenbal, J.C., Dortland, S., Gunnink, J.L., 2006. A comprehensive seismic velocity model for the Netherlands based on lithostratigraphic layers. Netherlands Journal of Geosciences 85(4), 277-292.

Yilmaz, O., 2001. Seismic Data Analysis: Processing, Inversion and Interpretation of Seismic Data. Society of Exploration Geophysicists, vols. 1-2. Tulsa, U.S.A.

Zanchi, A., Salvi, F., Zanchetta, S., Sterlacchini, S., Guerra, G., 2009. 3D reconstruction of complex geological bodies: Examples from the Alps. Computers & Geosciences 35(1), 49-69. doi:10.1016/j.cageo. 2007.09.003

Figure captions

Fig. 1 - 3D model production workflow. The dashed box titled "3D time-depth converter*" refers to the Vel-IO 3D flowchart in Fig. 6.

Fig. 2 - A) Regional stratigraphic scheme for the central Po Plain: horizon names refer to unit tops or unconformity surfaces. Lithostratigraphic unit codes used in 3D geological model and formation names from literature are also provided. The velocity layer-cake scheme, used for the velocity model, groups the lithostratigraphic units in four layers and distinguishes main key horizons. v_0 and k are respectively the initial velocity at the top of the considered layer and the gradient describing the velocity variations with depth. B) Sonic log and interval velocity plot of the Solarolo 001 well (see Fig. 8B for the location), this latter shows scattered velocity values and velocity reversals with depth.

Fig. 3 - Seismic reflection line interpretation. Black dashed lines represent the horizons (unit top or unconformity surface), red dashed lines represent faults. Refer to Fig. 2A for horizon codes, and to Fig. 8B for the location. (Seismic line is published thanks to ENI S.p.A. courtesy).

Fig. 4 - Nodes and meshes before (Time domain, upper part) and after (Depth domain, lower part) time-depth conversion procedure; location of points and boundaries are preserved. A) Perspective view; B) Map view.

Fig. 5 - A) Schematic example of well log velocity analysis. B) 2D example of instantaneous velocity model; *a* and *b* are two points located in intermediate position within the velocity model layer-cake. v_0 and k are respectively the initial velocity and the velocity gradient of each layer, twt is the two-way traveltime, Z is the depth after time-depth conversion, numbers in bolt and in subscript refer to the layers in the velocity model.

Fig. 6 - Simplified flowchart for Vel-IO 3D tool. For detailed Script schemes and flowcharts see Supplementary materials 1, Figs. S1, S2 and S3.

Fig. 7 - Simplified schema for Script 2 – Velocity model optimization. v_0, k, twt are respectively the initial velocity, the velocity gradient and the two-way traveltime of each layer (number in subscript); Z is the calculated depth (after the run of Script 1), Z_{cp} is the measured depth of marker corresponding to the key horizon at control point.

Fig 8 - A) Schematic structural map of the Po Plain (structural elements from Bigi et al., 1992 and Rossi et al., 2015). B) Structural scheme and dataset (ENI S.p.A. courtesy) of the study area. The white polygon represents the study area; the white dashed lines represent the location of 3D model slices in Fig. 10.

Fig. 9 - Maps of velocity parameters (v_0 and k) interpolated at the top of the four layers of the velocity model; they produced as output of Script 1 and/or Script 2. The black dots indicate the position and number of the wells and pseudo-wells with velocity data. In the study area, no barriers have been considered for the interpolation at the top of the Layer 4 (the deepest) due to the low number of input data.

Fig. 10 - Slice views of the 3D model (see Fig. 8B for the location). A) view from E; B) view from NW; C) view from W. Thrusts in purple have L1 detachment level, thrusts in red have L2 detachment level, extensional faults are in orange. Refer to Fig. 2A for horizon codes.

Fig. 11 - A) Comparison between the isobaths of the PL horizon in the GeoMol model and the Base of Pliocene in the Structural Model of Italy (Bigi et al., 1992). B) Absolute difference between the horizons of fig. 11 A. C) Cross section with the comparison of the two horizons of Fig 11 A.

Supplementary materials

Fig. S1 – Schematic flowchart algorithm of Script 1 – Velocity model builder. Config1.ini is the configuration file with input data and parameters; i is the iterator used in "*while*" loops; l is the number of loops to perform; v_0 (m/sec) and k (1/sec) are the velocity parameters; T_n (msec) is the two-way traveltime value at each point, T_{n-1} is the two-way traveltime value of the horizon directly above the considered point; Z_{n-1} (meters) is the value of depth in meters of the horizon directly above the considered point; Z_n is the depth of the considered point.

Fig. S2 – Schematic flowchart algorithm of Script 2 – Velocity model optimizer. Config2.ini is the configuration file with input data and parameters; i is the iterator used in "*while*" loops; l is the number of loops to perform; v_0 (m/sec) and k (1/sec) are the velocity parameters; Z_n (meters) is the depth of the considered point; "steps" is the number of subdivisions of the standard deviation range used to discretize the optimization analysis; "EOD" is end of data; $Z=f(v_0,k)$ is the simplified form for the Marsden equation; $\Delta=Z-Z_{cp}$ is the difference between the calculated depth (Z) and the measured depth at each control point (Z_{cp}); min Δ is the minimum value of Δ; tolerance (in meters) is the threshold for warnings.

Fig. S3 – Schematic flowchart algorithm of Script 3 – Time-Depth converter. Config3.ini is the configuration file with input data and parameters; v_0 (m/sec) and k (1/sec) are the velocity parameters; twt is the two-way traveltime (msec); Z is the depth in meters; "EOD" is end of data; Tl is the two-way traveltime of the deepest key horizon at the coordinates of the considered point; T1 is the two-way traveltime of the uppermost key horizon at the coordinates of the considered point; a is an iterator used to explore the intermediate layers; Ta and Ta-1 are the two-way time values of layer a and a-1 respectively at the coordinate of the considered point.

Highlights

- A comprehensive 3D geological modeling workflow for wide flat regions is proposed

- Vel-IO 3D tool allows 3D instantaneous velocity model construction and optimization
- Vel-IO 3D includes time-depth conversion of the 3D geological models in time domain
- The workflow is tested in a wide flat structurally complex area in the Po Plain